JCB Article

YHR150w and *YDR479c* encode peroxisomal integral membrane proteins involved in the regulation of peroxisome number, size, and distribution in *Saccharomyces cerevisiae*

Franco J. Vizeacoumar,[1] Juan C. Torres-Guzman,[1,2] Yuen Yi C. Tam,[1] John D. Aitchison,[1,3] and Richard A. Rachubinski[1]

[1]Department of Cell Biology, University of Alberta, Edmonton, Alberta T6G 2H7, Canada
[2]Instituto de Investigaciones en Biologiá Experimental, University of Guanajuato, Guanajuato, Mexico
[3]The Institute for Systems Biology, Seattle, WA 98103

The peroxin Pex24p of the yeast *Yarrowia lipolytica* exhibits high sequence similarity to two hypothetical proteins, Yhr150p and Ydr479p, encoded by the *Saccharomyces cerevisiae* genome. Like *Yl*Pex24p, both Yhr150p and Ydr479p have been shown to be integral to the peroxisomal membrane, but unlike *Yl*Pex24p, their levels of synthesis are not increased upon a shift of cells from glucose- to oleic acid–containing medium. Peroxisomes of cells deleted for either or both of the *YHR150w* and *YDR479c* genes are increased in number, exhibit extensive clustering, are smaller in area than peroxisomes of wild-type cells, and often exhibit membrane thickening between adjacent peroxisomes in a cluster. Peroxisomes isolated from cells deleted for both genes have a decreased buoyant density compared with peroxisomes isolated from wild-type cells and still exhibit clustering and peroxisomal membrane thickening. Overexpression of the genes *PEX25* or *VPS1*, but not the gene *PEX11*, restored the wild-type phenotype to cells deleted for one or both of the *YHR150w* and *YDR479c* genes. Together, our data suggest a role for Yhr150p and Ydr479p, together with Pex25p and Vps1p, in regulating peroxisome number, size, and distribution in *S. cerevisiae*. Because of their role in peroxisome dynamics, *YHR150w* and *YDR479c* have been designated as *PEX28* and *PEX29*, respectively, and their encoded peroxins as Pex28p and Pex29p.

Introduction

Peroxisomes, together with the glyoxysomes of plants and glycosomes of trypanosomes, make up the microbody family of organelles. Peroxisomes play diverse roles in the cell, compartmentalizing many activities related to lipid metabolism and functioning in the decomposition of toxic hydrogen peroxide (for reviews see Lazarow and Fujiki, 1985; van den Bosch et al., 1992; Subramani, 1993; Titorenko and Rachubinski, 2001).

Proteins destined for the peroxisomal matrix are synthesized on free polyribosomes and are imported posttranslationally (Lazarow and Fujiki, 1985; Subramani 1993, 1998; Subramani et al., 2000; Purdue and Lazarow, 2001). Most peroxisomal matrix proteins are sorted by tripeptide peroxisome-targeting signal 1 (PTS1)* located at their carboxy termini (Gould et al., 1987, 1989, 1990; Aitchison et al., 1991; Swinkels et al., 1992), whereas a limited subset of proteins are sorted by a nonapeptide PTS2 at their amino termini (Osumi et al., 1991; Swinkels et al., 1991; Glover et al., 1994b; Waterham et al., 1994). A few exceptional matrix proteins are targeted by internal PTSs, which remain largely uncharacterized (Small et al., 1988; Purdue et al., 1990; Kragler et al., 1993; Elgersma et al., 1995).

Pex5p and Pex7p are receptors specific for PTS1- and PTS2-containing proteins, respectively. These receptors are mobile, interacting with their cargo in the cytosol and docking

The online version of this article includes supplemental material.

Address correspondence to Richard A. Rachubinski, Department of Cell Biology, University of Alberta, Medical Sciences Building 5-14, Edmonton, Alberta T6G 2H7, Canada. Tel: (780) 492-9868. Fax: (780) 492-9278. E-mail: rick.rachubinski@ualberta.ca

Key words: biogenesis; peroxin; protein similarity; open reading frame; membrane fission

*Abbreviations used in this paper: DsRed, *Discosoma sp*. red fluorescent protein; PBD, peroxisome biogenesis disorder; PNS, postnuclear supernatant; PTS1, peroxisome-targeting signal 1; SM, synthetic minimal.

© The Rockefeller University Press, 0021-9525/2003/04/321/12 $8.00

The Journal of Cell Biology

at the peroxisomal membrane through interaction with Pex13p and Pex14p (for reviews see Subramani, 1998; Hettema et al., 1999; Terlecky and Fransen, 2000; Purdue and Lazarow, 2001; Titorenko and Rachubinski, 2001). Strikingly, the PTS1 receptor has been shown to enter the peroxisomal matrix together with its cargo and to recycle back to the cytosol after dissociation from its cargo (Dammai and Subramani, 2001). The recycled PTS1 receptor is then available for another round of peroxisomal matrix protein import. The pathway of targeting of peroxisomal membrane proteins remains relatively uncharacterized, although it appears to be independent of the pathway of matrix protein targeting. Stretches of basic amino residues on the matrix side of membrane proteins, close to a transmembrane sequence, have been proposed to act in targeting proteins to the peroxisomal membrane (McCammon et al., 1994; Dyer et al., 1996; Elgersma et al., 1997; Pause et al., 2000).

A remarkable feature of peroxisomal protein import is that folded and assembled multimeric proteins can enter the organelle (Walton et al., 1992, 1995; Glover et al., 1994a; McNew and Goodman, 1994). The oligomerization of some of these multimeric proteins is facilitated by specific chaperone molecules, as in the case of the soluble peroxisomal matrix protein thiolase and its chaperone Pex20p (Titorenko et al., 1998), or is self-assisted, as in the case of the heteropentameric fatty acyl–CoA oxidase complex of the yeast *Yarrowia lipolytica* (Titorenko et al., 2002).

Failure to assemble functional peroxisomes leads to a class of genetic diseases known as the peroxisome biogenesis disorders (PBDs), the archetype of which is Zellweger syndrome (Lazarow and Moser, 1994; Brosius and Gärtner, 2002). Defining the molecular basis of the PBDs has been an area of intense research in recent years, particularly in regards to the identification of the genes controlling peroxisome assembly, the so called *PEX* genes. Of the 25 *PEX* genes identified so far, mutations in 11 of the 13 human orthologues have been shown to cause PBDs (for reviews see Fujiki, 2000; Gould and Valle, 2000; Subramani et al., 2000; Brosius and Gärtner, 2002). The identification of additional genes involved in peroxisome assembly and elucidation of the roles of the proteins they encode would provide greater understanding of the molecular basis of these lethal disorders. The completion of the *Saccharomyces cerevisiae* genome sequencing project has increased the utility of this model organism for the identification of novel genes involved in peroxisome assembly. Microarray transcriptional profiling of *S. cerevisiae* under conditions of peroxisome induction has already led to the identification of a novel *PEX* gene, *PEX25* (Smith et al., 2002), and knowledge of the entire coding capacity of the *S. cerevisiae* genome has facilitated the identification of new proteins potentially involved in peroxisome assembly by their similarity with other proteins already shown to be involved in peroxisome assembly in other organisms.

We recently reported the isolation and characterization of *Yl*Pex24p, a 61-kD integral membrane protein of peroxisomes required for peroxisome assembly in *Y. lipolytica* (Tam and Rachubinski, 2002). A search of protein databases revealed that *Yl*Pex24p shares extensive sequence similarity with proteins encoded by the ORFs *YHR150w* and *YDR479c* of the *S. cerevisiae* genome. Here we report that both *YHR150w* and *YDR479c* code for peroxisomal integral membrane proteins, and we provide evidence for their role in peroxisomal dynamics in *S. cerevisiae*.

Results

Yhr150p and Ydr479p share extensive similarity with *Y. lipolytica* Pex24p

*Yl*Pex24p is an integral peroxisomal membrane protein that has been shown to be required for peroxisome assembly in the yeast *Y. lipolytica* (Tam and Rachubinski, 2002). A search of protein databases with the GENEINFO(R) BLAST Network Service of the National Center for Biotechnology Information revealed two proteins encoded by the ORFs *YHR150w* and *YDR479c* of the *S. cerevisiae* genome that exhibit extensive sequence similarity to *Yl*Pex24p (Fig. 1). *Yl*Pex24p and Yhr150p exhibit 21.1% amino acid

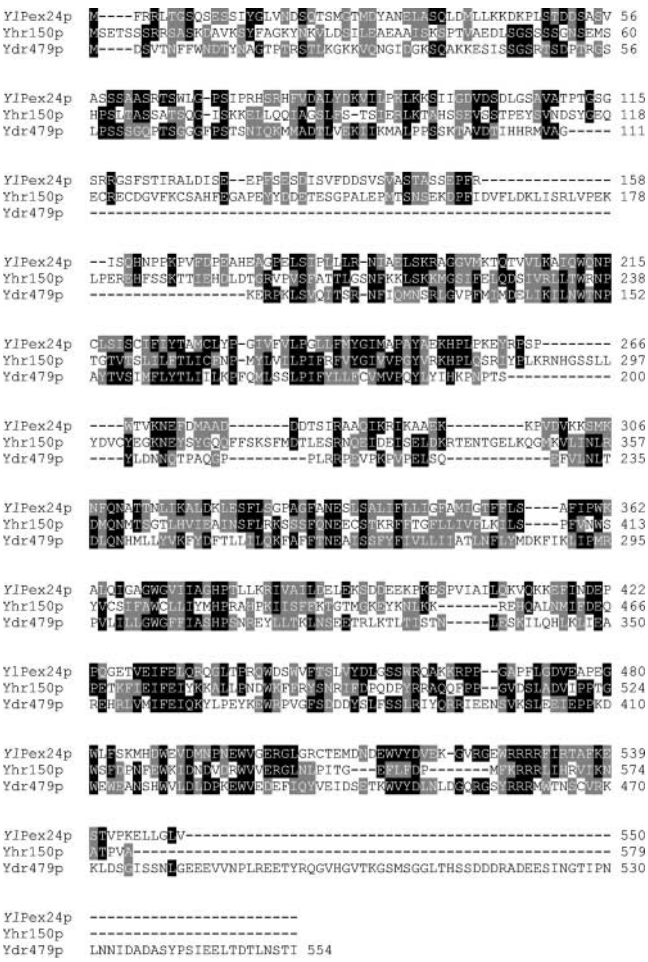

Figure 1. **Sequence alignment of *Yarrowia lipolytica* Pex24p with the proteins Yhr150p and Ydr479p encoded by the *Saccharomyces cerevisiae* genome.** Amino acid sequences were aligned with the use of the ClustalW program (EMBL European Bioinformatics Institute, http://www.ebi.ac.uk/clustalw/). Identical residues (black) and similar residues (gray) in at least two of the proteins are shaded. Similarity rules: G = A = S; A = V; V = I = L = M; I = L = M = F = Y = W; K = R = H; D = E = Q = N; and S = T = Q = N. Dashes represent gaps.

The Journal of Cell Biology

identity and 44.4% amino acid similarity, *Yl*Pex24p and Ydr479p exhibit 20.8% amino acid identity and 42.1% amino acid similarity, while Yhr150p and Ydr479p exhibit 20.4% amino acid identity and 41.3% amino acid similarity. Yhr150p is predicted to be a protein of molecular weight 66,145 and to have two transmembrane helices at amino acids 246–268 and 393–415 (http://www.cbs.dtu.dk/services/TMHMM-2.0/) (Krogh et al., 2001). Ydr479p is predicted to be a protein of molecular weight 63,533 and to have four transmembrane helices at amino acids 146–165, 172–194, 265–284, and 291–308. Some potential functional redundancy between Yhr150p and Ydr479p may have prevented them from being identified as being involved in peroxisome assembly in *S. cerevisiae* by procedures involving random mutagenesis and negative selection for growth of yeast on oleic acid–containing medium.

Synthesis of Yhr150p and Ydr479p remains constant during incubation of cells in oleic acid–containing medium

The synthesis of many peroxisomal proteins is induced by the incubation of yeast cells in oleic acid-containing medium. Genomically encoded protein A chimeras of Yhr150p and Ydr479p were monitored to analyze the expression of *YHR150w* and *YDR479c*, respectively, under the control of their endogenous gene promoters. Yeast strains synthesizing Yhr150p-prA, Ydr479p-prA, thiolase-prA, and Pex17p-prA were grown in glucose-containing YPD medium and then shifted to oleic acid–containing YPBO medium. Aliquots of cells were removed at various times after the shift to YPBO medium, and their lysates were subjected to SDS-PAGE and immunoblotting (Fig. 2). Yhr150p-prA and Ydr479-prA, as well as Pex17p-prA (Huhse et al., 1998), were detected in glucose-containing YPD medium at the time of transfer, and their respective levels did not increase with time of incubation of cells in YPBO medium. In contrast, thiolase-prA was barely detectable in cells at the time of transfer to YPBO medium, and its levels were substantially increased with time of incubation in YPBO medium.

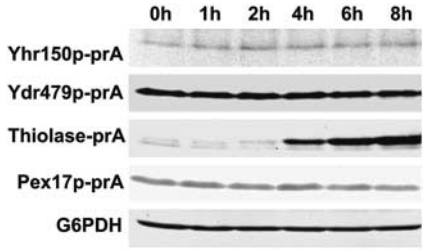

Figure 2. **Yhr150p-prA and Ydr479p-prA remain at constant levels during incubation of *S. cerevisiae* in oleic acid–containing medium.** Cells were grown for 16 h in glucose-containing YPD medium and then transferred to, and incubated in, oleic acid–containing YPBO medium. Aliquots of cells were removed from the YPBO medium at the times indicated, and total cell lysates were prepared. Equal amounts of protein from the total cell lysates were analyzed by SDS-PAGE and immunoblotting to visualize the protein A fusions. Antibodies directed against glucose-6-phosphatase (G6PDH) were used to confirm the loading of equal protein in each lane.

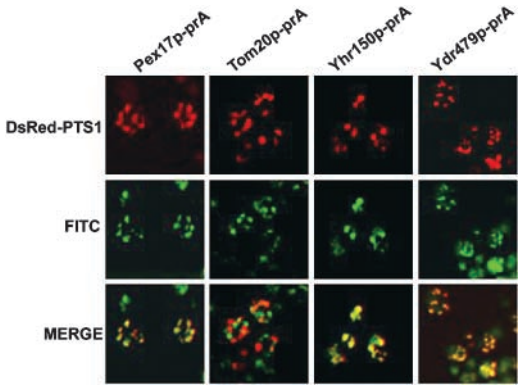

Figure 3. **Yhr150p-prA and Ydr479p-prA are peroxisomal proteins by microscopy.** The subcellular distributions of protein A chimeras were compared with that of DsRed–PTS1 in oleic acid–incubated cells by double labeling, indirect immunofluorescence microscopy. Yhr150p-prA and Ydr479p-prA colocalize with DsRed–PTS1 in punctate structures characteristic of peroxisomes. There is no colocalization of DsRed–PTS1 and the protein A chimera of the mitochondrial protein Tom20p. Protein A chimeras were detected with rabbit antibodies to mouse IgG and FITC-conjugated goat anti–rabbit IgG secondary antibodies.

Yhr150p and Ydr479p are primarily integral membrane proteins of peroxisomes

A carboxy-terminal PTS1 is sufficient to direct a reporter protein to peroxisomes (for review see Purdue and Lazarow, 2001). A fluorescent chimera between *Discosoma sp.* red fluorescent protein (DsRed) and the PTS1 Ser-Lys-Leu has been shown to target to peroxisomes of *S. cerevisiae* (Smith et al., 2002). Genomically encoded protein A chimeras of Yhr150p, Ydr479p, the peroxisomal peroxin Pex17p, (Huhse et al., 1998) and the mitochondrial translocon protein Tom20p (Lithgow et al., 1994) were localized in oleic acid–induced cells by indirect immunofluorescence microscopy combined with direct fluorescence from DsRed–PTS1 to identify peroxisomes (Fig. 3). Yhr150p-prA, Ydr479p-prA, and Pex17p-prA colocalized with DsRed–PTS1 to small punctate structures characteristic of peroxisomes by confocal microcopy. As expected, Tom20p-prA did not colocalize with DsRed–PTS1, as the respective individual green and red signals for these proteins remained separate in confocal microscopy.

Subcellular fractionation and organelle extraction were used to establish if Yhr150p and Ydr479p are associated with peroxisomes and to determine their suborganellar locations. Cells expressing Yhr150p-prA, Ydr479p-prA, and Pex17p-prA were incubated in oleic acid–containing medium and subjected to subcellular fractionation to yield postnuclear supernatant (PNS) fractions. The PNS fractions were subjected to further centrifugation to yield a supernatant fraction (20KgS) enriched for cytosol and a crude organellar pellet fraction (20KgP). Equal portions of the PNS, 20KgS, and the 20KgP were analyzed by immunoblotting. Yhr150p-prA, Ydr479p-prA, and Pex17p-prA all preferentially localized to the 20KgP fraction (Fig. 4 A). Peroxisomes were isolated from the 20KgP fractions of each of the strains expressing Yhr150p-prA, Ydr479p-prA, and Pex17p-prA. The gradients were fractionated, and equal portions of each fraction were analyzed by immunoblotting (Fig. 4 B). Yhr150p-prA and Ydr479p-prA coenriched with the peroxi-

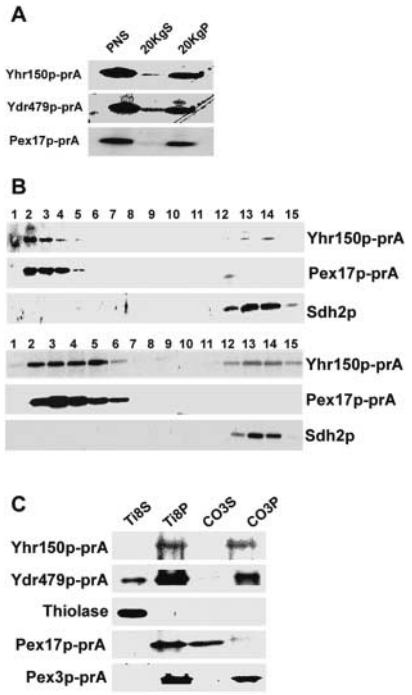

Figure 4. **Yhr150p-prA and Ydr479p-prA are primarily integral peroxisomal membrane proteins.** (A) A PNS fraction was divided by centrifugation into a supernatant (20KgS) fraction enriched for cytosol and a pellet (20KgP) fraction enriched for peroxisomes and mitochondria. Equivalent portions of each fraction were analyzed. Immunoblotting detected the protein A chimeras shown, including that of the peroxisomal protein Pex17p. (B) Yhr150p-prA and Ydr479p-prA cofractionate with peroxisomes. Organelles in the 20KgP fraction were separated by isopycnic centrifugation on a discontinuous Nycodenz gradient. Fractions were collected from the bottom of the gradient, and equal portions of each fraction were analyzed by immunoblotting. Fractions enriched for peroxisomes and mitochondria were identified by immunodetection of the protein A chimera of Pex17p and Sdh2p, respectively. (C) Peroxisomes purified by isopycnic density gradient centrifugation were lysed by treatment with 10 mM Tris-HCl, pH 8.0, releasing matrix proteins to a supernatant fraction (Ti8S) after centrifugation. The membrane-containing pellet fraction (Ti8P) was treated with 0.1 M Na_2CO_3, pH 11.3, and then subjected to centrifugation to yield a supernatant fraction (CO3S) enriched for peripherally associated membrane proteins and a pellet fraction (CO3P) enriched for integral membrane proteins. Equal portions of the respective supernatant and pellet fractions were analyzed by immunoblotting. Immunodetection of thiolase, Pex17p-prA, and Pex3p-prA marked the fractionation profiles of a matrix, peripheral membrane, and integral membrane protein, respectively.

somal peroxin Pex17p-prA and not with the mitochondrial protein, Sdh2p. Therefore, both microscopic analysis and subcellular fractionation showed Yhr150p and Ydr479p to be peroxisomal proteins. Some amount of Ydr479p-prA was always present in the 20KgS fraction and in the lighter fractions during the gradient isolation of peroxisomes. Whether this represents a selective liberation of a soluble form of Ydr479p-prA during the isolation of peroxisomes remains undetermined. It is unlikely that Ydr479p-prA is found in a cellular compartment in addition to peroxisomes, as immunostaining for Ydr479p-prA yielded exclusively a punctate pattern corresponding to the punctate pattern of peroxisomes defined by DsRed–PTS1 (Fig. 3). In addition, this punctate compartment does not correspond to mitochondria, as the fluorescence pattern generated with the mitochondria-specific dye MitoTracker did not overlap with the punctate pattern generated by detection of Ydr479p-prA by immunofluorescence (unpublished data).

Peroxisomes were hypotonically lysed by incubation in dilute alkali Tris buffer and subjected to centrifugation to yield a supernatant (Ti8S) enriched for matrix proteins and a pellet (Ti8P) enriched for membrane proteins (Fig. 4 C). The chimeras of Yhr150p and Ydr479p localized primarily to the Ti8P fraction, as did the chimeras of the peripheral peroxisomal membrane protein Pex17p (Huhse et al., 1998) and the integral peroxisomal membrane protein Pex3p (Höhfeld et al., 1991). The soluble peroxisomal matrix protein thiolase was found almost exclusively in the Ti8S fraction. The reproducible presence of some Ydr479p in the Ti8S fraction may again be representative of a soluble form of this protein that is selectively liberated during the isolation of peroxisomes (Fig. 4, A and B). The Ti8P fractions were then extracted with alkali sodium carbonate and subjected to centrifugation (Fig. 4 C). This treatment releases proteins associated with, but not integral to, membranes (Fujiki et al., 1982). Under these conditions, Yhr150p-prA and Ydr479p-prA fractionated with Pex3p-prA to the pellet fraction enriched for integral membrane proteins, whereas Pex17p-prA fractionated to the supernatant fraction enriched for soluble proteins, including peripheral membrane proteins. These data suggest that Yhr150p and Ydr479p are both primarily integral peroxisomal membrane proteins, as has been shown for *Yl*Pex24p (Tam and Rachubinski, 2002).

Cells deleted for either or both of the *YHR150w* and *YDR479c* genes contain increased numbers of smaller peroxisomes that exhibit clustering

We next investigated the ultrastructure of cells incubated in oleic acid–containing YPBO medium by transmission EM. Wild-type cells (Fig. 5 A) consistently showed individual peroxisomes well separated from one another. In contrast, cells of the *yhr150Δ* (Fig. 5 B), *ydr479Δ* (Fig. 5 C), and, particularly, *yhr150Δ/ydr479Δ* (Fig. 5 D) strains contained peroxisomes that exhibited clustering. 28.0, 19.2, and 20.4% of peroxisomes of cells of the *yhr150Δ/ydr479Δ*, *ydr479Δ*, and *yhr150Δ* strains, respectively, showed clustering, in contrast to 4.0% of peroxisomes of wild-type cells (a cluster of peroxisomes was operationally defined as three or more adherent peroxisomes). The clustered peroxisomes often showed evidence of membrane thickening between adjacent peroxisomes in the cluster. Morphometric analysis showed that cells of the deletion strains contained a greater number of peroxisomes than wild-type cells and that, on average, these peroxisomes were smaller in size than those of wild-type cells (Table I). Cells of the deletion strains contained much greater numbers of peroxisomes with areas of 0.02 μm^2 or less than wild-type cells (Fig. 5 E). Nycodenz density gradient centrifugation analysis showed that peroxisomes purified from *yhr150Δ/ydr479Δ* cells have a greatly reduced density (peak fraction 8, 1.19 g/cm^3) compared with peroxisomes from wild-type cells (peak fraction 1, 1.22 g/cm^3) (Fig. 6 A). Peroxisomes isolated from cells deleted for *YHR150w* or *YDR479c* were also less dense than wild-type

The Journal of Cell Biology

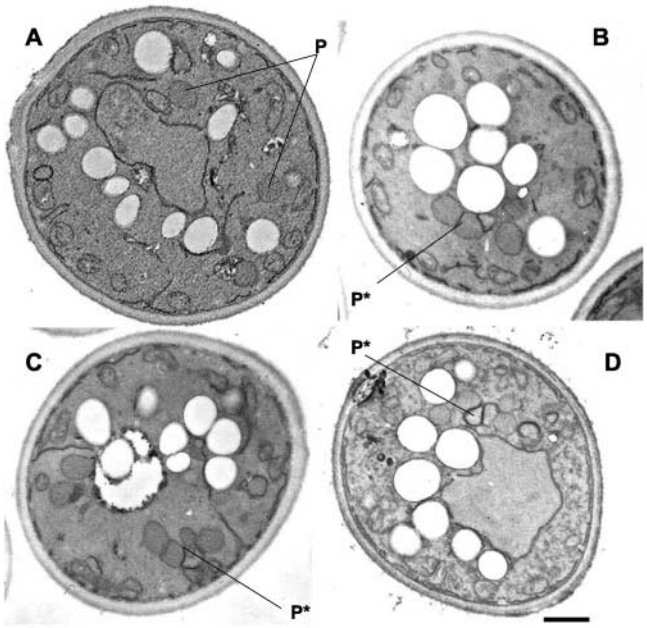

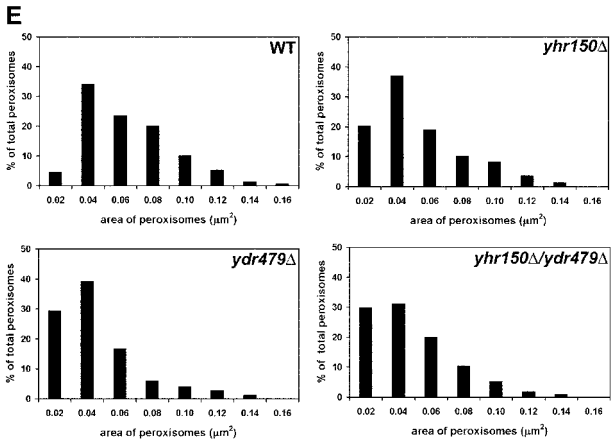

Figure 5. **Peroxisomes are smaller, more abundant, and exhibit clustering in cells deleted for either or both of the *YHR150w* and *YDR479c* genes.** Ultrastructure of wild-type *BY4742* (A), *yhr150Δ* (B), *ydr479Δ* (C), and *yhr150Δ/ydr479Δ* (D) cells. Cells were grown in YPD medium overnight, transferred to YPBO medium, and incubated in YPBO medium for 8 h. Cells were fixed and processed for EM. P, peroxisome; P*, peroxisome cluster. Bar, 0.5 μm. (E) Morphometric analysis of peroxisomes of oleic acid–incubated wild-type (*WT*) *BY4742* and deletion mutant cells. For each strain analyzed, electron micrographs of 50 randomly selected cells at a magnification of 17,000 were scanned, and the areas of individual peroxisomes were determined by counting the number of individual pixels in a peroxisome with Image Tools for Windows, Version 2.00. The peroxisomes were then separated into size categories. A histogram was generated for each strain depicting the percentage of total peroxisomes occupied by the peroxisomes of each category. The numbers along the x axis are the maximum sizes of peroxisomes in each category (in μm^2).

peroxisomes, although the differences in density were less than that observed between peroxisomes from *yhr150Δ/ydr479Δ* cells and wild-type peroxisomes (unpublished data). EM analysis showed that the peroxisomes purified from *yhr150Δ/ydr479Δ* cells still exhibited clustering and evidence of thickened peroxisomal membranes, whereas peroxisomes purified from wild-type cells were largely well separated from one another, with no evidence of membrane thickening (Fig. 6 B).

Overexpression of *PEX25* or *VPS1*, but not *PEX11*, restores wild-type peroxisome morphology to cells deleted for one or both of the *YHR150w* and *YDR479c* genes

Because cells deleted for one or both of the *YHR150w* and *YDR479c* genes are compromised in their regulation of peroxisome number, size, and distribution, we investigated the effects of overexpression of three genes previously shown to be involved in these processes in *S. cerevisiae*. Cells of strains mutant for the genes encoding the peroxisomal peroxins Pex11p (Erdmann and Blobel, 1995; Marshall et al., 1995, 1996), Pex25p (Smith et al., 2002), and the dynamin-like protein Vps1p (Hoepfner et al., 2001) have reduced numbers of enlarged peroxisomes compared with wild-type cells (see Fig. S1, available at http://www.jcb.org/cgi/content/full/jcb.200210130/DC1). Overexpression of *PEX25* (Fig. 7; Fig. 8 D) or *VPS1* (Fig. 7; Fig. 8 E) in cells deleted for one or both of the *YHR150w* and *YDR479c* genes led to a partial restoration of the wild-type peroxisomal phenotype, with overexpressing cells containing increased numbers of separate, individual peroxisomes and reduced numbers of peroxisomal clusters (see Figs. S5 and S6, available at http://www.jcb.org/cgi/content/full/jcb.200210130/DC1). In contrast, overexpression of *PEX11* did not appear to have any effect on the abnormal peroxisome morphology observed in cells mutant for the *YHR150w* and *YDR479c* genes (Fig. 7; Fig. 8 C; Fig. S4, available at http://www.jcb.org/cgi/content/full/jcb.200210130/DC1). It should be noted that overexpression of the *YHR150w* gene led to restoration of wild-type peroxisome morphology in

Table I. **Average area and numerical density of peroxisomes in cells of wild-type and deletion strains**

Strain	Cell area assayed	Peroxisome count[a]	Numerical density of peroxisomes[b]	Average area of peroxisomes[c]
	μm^2			μm^2
WT (BY4742)	404	0.37	1.71	0.055
yhr150Δ	424	0.51	2.59	0.048
ydr479Δ	382	0.56	3.20	0.039
yhr150Δ/ydr479Δ	381	0.80	4.38	0.040

[a]Number of peroxisomes counted per μm^2 of cell area on micrographs.
[b]Number of peroxisomes per μm^3 of cell volume (Weibel and Bolender, 1973).
[c]Average area on micrographs.

The Journal of Cell Biology

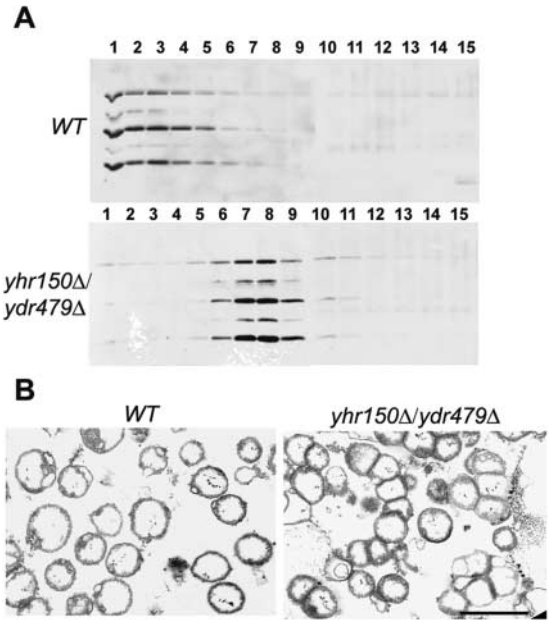

Figure 6. **Peroxisomes isolated from *yhr150Δ/ydr479Δ* cells are less dense than isolated wild-type peroxisomes and retain a clustered phenotype.** (A) The wild-type (*WT*) strain *BY4742* and the mutant strain *yhr150Δ/ydr479Δ* were grown overnight in YPD medium, transferred to oleic acid–containing YPBO medium, and incubated in YPBO medium for 8 h. A PNS fraction was prepared from cells of each strain and divided by centrifugation into 20KgS and 20KgP fractions. Organelles in the 20KgP fraction were separated by isopycnic centrifugation on a continuous 30–45% Nycodenz gradient. Fractions were collected from the bottom of the gradient, and equal portions of each fraction were analyzed by immunoblotting with antibodies to the PTS1, Ser-Lys-Leu, to detect peroxisomes. (B) Electron micrographs of peak peroxisomal fractions from cells of the wild-type strain (*WT*) *BY4742* (fraction 1) and the mutant strain *yhr150Δ/ydr479Δ* (fraction 8). Bar, 0.5 μm.

yhr150Δ cells but not in *ydr479Δ* cells or in cells deleted for both the *YHR150w* and *YDR479c* genes (Fig. 7, Fig. 8 A; Fig. S2, available at http://www.jcb.org/cgi/content/full/jcb.200210130/DC1). In contrast, overexpression of *YDR479c* led to restoration of wild-type peroxisome morphology not only in *ydr479Δ* cells, but also in *yhr150Δ* cells and cells deleted for both genes (Fig. 7; Fig. 8 B; Fig. S3, available at http://www.jcb.org/cgi/content/full/jcb.200210130/DC1). Therefore, it appears that Yhr150p may be, for the most part, redundant in its functions in regulating peroxisome dynamics with respect to Ydr479p. Attempts at demonstrating physical interactions, either direct or indirect, between Yhr150p and Ydr479p or between these two proteins and Pex11p, Pex25p, or Vps1p were unsuccessful (unpublished data).

As reported previously (Erdmann and Blobel, 1995; Marshall et al., 1995, 1996; Hoepfner et al., 2001; Smith et al., 2002), cells deleted individually for the *PEX11*, *PEX25*, and *VPS1* genes contained reduced numbers of enlarged peroxisomes (Fig. 7; Fig. S1). Overexpression of the *PEX11* gene in wild-type cells or in cells deleted for *PEX11*, *PEX25*, or *VPS1* led to a proliferation of smaller peroxisomes (Fig. 7; Fig. S4). However, overexpression of *PEX25* or *VPS1*, although resulting in normal peroxisome morphology in their respective mutant backgrounds, did not affect the peroxisome morphology in the opposite mutant background (Fig. 7; Figs. S5 and S6). Overexpression of *PEX25*, but not *VPS1*, led to only a nominal increase in the number of normal peroxisomes in cells deleted for the *PEX11* gene (Fig. 7; Figs. S5 and S6). Moreover, the *pex11Δ* cells retained their enlarged peroxisomal phenotype when either *YHR150w* or *YDR479c* was overexpressed (Fig. 7; Figs. S2 and S3). Our results suggest that Pex11p plays a central role in regulating peroxisome division. The results of gene overexpression studies are summarized in Table II.

Discussion

Completion of the *S. cerevisiae* genome sequencing project proved invaluable for the identification of a novel *PEX* gene, *PEX25*, by transcriptome profiling of cells grown in oleic acid–containing medium versus cells grown in glucose-containing medium (Smith et al., 2002). The completed *S. cerevisiae* genome sequence has added value in that it provides the opportunity to identify novel proteins required for peroxisome biogenesis in *S. cerevisiae* through sequence similarity between proteins of unknown function encoded by *S. cerevisiae* and proteins already shown to be required for peroxisome biogenesis in other organisms. We recently demonstrated the requirement of the peroxisomal integral membrane protein Pex24p for peroxisome assembly in the yeast *Y. lipolytica* (Tam and Rachubinski, 2002). *Yl*Pex24p was shown to share extensive sequence similarity with two proteins of unknown function and unknown localization encoded by the ORFs *YHR150w* and *YDR479c* of the *S. cerevisiae* genome. In this manuscript, genomically encoded protein A chimeras of Yhr150p and Ydr479p were shown by a combination of microscopic and subcellular fractionation analyses to be peroxisomal proteins. In their response to extraction by different salts, Yhr150p and Ydr479p act primarily as integral membrane proteins. However, a fraction of Ydr479p consistently acts as a soluble protein. The exact nature of this soluble form of Ydr479p and its origin (is it in equilibrium with the peroxisomal membrane form of Ydr479p?) remain under investigation.

The proteins encoded by the *YHR150w* and *YDR479c* genes are not required for peroxisome assembly, as cells harboring deletions for one or both of these genes still contain peroxisomes. These peroxisomes were functional, at least to some degree, as the cells containing one or both of the gene deletions were able to grow in oleic acid–containing medium with essentially the same kinetics as the wild-type strain (unpublished data). However, the peroxisomes in the deleted strain are not normal and show phenotypic characteristics distinct from those of wild-type peroxisomes. The peroxisomes of cells deleted for one or both of the *YHR150w* and *YDR479c* genes are more abundant, smaller, and show extensive clustering, as compared with wild-type peroxisomes. In addition, the membranes of the clustered peroxisomes of the gene deletion strains are often thickened in appearance. These characteristics of peroxisomes of the deletion strains are consistent with a role for *YHR150w* and *YDR479c* in the control of peroxisome size, number, and distribution within cells. However, it does not appear that

The Journal of Cell Biology

Table II. **Summary of results of gene overexpression**

	Normal peroxisomes	Clustered peroxisomes	Enlarged peroxisomes
YHR150w overexpression in			
Wild type	++++[a]		
yhr150Δ	++++		
ydr479Δ	+++	+	
yhr150Δ/ydr479Δ	++	++	
pex11Δ	+		+++
pex25Δ	+		+++
vps1Δ			++++
YDR479w overexpression in			
Wild type	++++		
yhr150Δ	++++		
ydr479Δ	++++		
yhr150Δ/ydr479Δ	++++		
pex11Δ	+		+++
pex25Δ	+		+++
vps1Δ			++++
PEX11 overexpression in			
Wild type	++	++	
yhr150Δ	+	+++	
ydr479Δ	+	+++	
yhr150Δ/ydr479Δ	+	+++	
pex11Δ	+	+++	
pex25Δ	++	+	+
vps1Δ	+	++	+
PEX25 overexpression in			
Wild type	++		++
yhr150Δ	++++		
ydr479Δ	++++		
yhr150Δ/ydr479Δ	+++	+	
pex11Δ	++		++
pex25Δ	++++		
vps1Δ			++++
VPS1 overexpression in			
Wild type	++++		
yhr150Δ	+++	+	
ydr479Δ	+++	+	
yhr150Δ/ydr479Δ	++	++	
pex11Δ	+		+++
pex25Δ	+		+++
vps1Δ	++++		
Controls			
Wild type	++++		
yhr150Δ	+	+++	
ydr479Δ	+	+++	
yhr150Δ/ydr479Δ	+	+++	
pex11Δ	+		+++
pex25Δ	+		+++
vps1Δ			++++

[a]The + symbol denotes the presence of a particular peroxisomal morphological phenotype. Increased numbers of + symbols denote increased prevalence of a particular peroxisomal morphological phenotype. The absence of a + symbol denotes the absence of a particular peroxisomal morphological phenotype.

YHR150w and *YDR479c* are required for peroxisome inheritance per se, as all cells deleted for one or both of these genes still contained peroxisomes after numerous cell divisions. Also, if *YHR150w* or *YDR479c* had a direct role in the inheritance of peroxisomes, one might expect that a loss of peroxisomes from cells over time resulting from impaired segregation of peroxisomes into daughter cells would lead to decreased kinetics of growth in oleic acid–containing medium for the deletion strains when compared to the wild-type strain, which, as reported above, was not observed. It is interesting to note that *Y. lipolytica* cells deleted for the *PEX24* gene also show evidence of abnormal peroxisomal divisional control. These cells lack mature peroxisomes but do accumulate membrane structures that contain both peroxi-

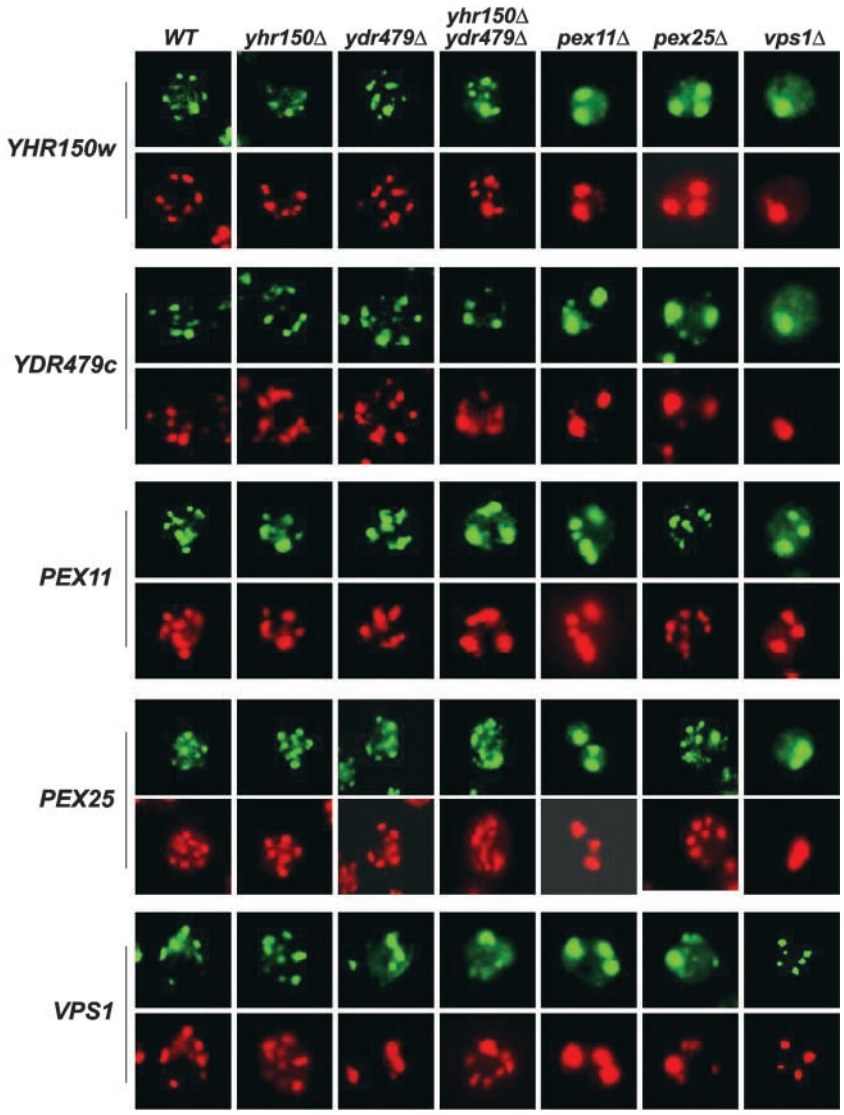

Figure 7. **Peroxisome morphology in cells of gene overexpression strains.** Cells were grown in SM medium overnight, transferred to YPBO medium, and incubated in YPBO medium for 8 h. Peroxisomes were detected by double labeling, indirect immunofluorescence microscopy with antibodies to the PTS1 Ser-Lys-Leu (SKL) and FITC-conjugated goat anti-rabbit IgG secondary antibodies, and with guinea pig antibodies to the PTS2-containing protein thiolase and rhodamine-conjugated donkey anti–guinea pig IgG secondary antibodies. The genetic backgrounds of the different yeast strains are given at the top, and the genes that are overexpressed are denoted on the left.

somal matrix and membrane proteins (Tam and Rachubinski, 2002). However, these membrane structures are not functional peroxisomes in *Y. lipolytica*, as *pex24Δ* cells cannot grow on medium containing oleic acid as the sole carbon source. Therefore, although *Yl*Pex24p, like Yhr150p and Ydr479p, most likely has a role in the regulation of peroxisome division, *Yl*Pex24p probably does not function identically to Yhr150p or Ydr479p, or is modulated in its actions differently than Yhr150p and Ydr479p.

The size, number, and distribution of peroxisomes are tightly controlled by the cell. Loss of the enzymatic activities of individual peroxisomal β-oxidation enzymes has been shown to result in pronounced changes in peroxisome size and/or number (Fan et al., 1998; Chang et al., 1999; Smith et al., 2000; van Roermund et al., 2000), due primarily to the increased levels of the remaining peroxisomal β-oxidation enzymes. The molecular mechanisms underlying this so-called metabolic control of peroxisome abundance (Chang et al., 1999) remain essentially unknown.

In contrast, members of the Pex11 family of peroxins have been implicated as effectors of peroxisome division in multiple species (Erdmann and Blobel, 1995; Marshall et al., 1995, 1996; Sakai et al., 1995; Abe and Fujiki, 1998; Lorenz et al., 1998; Passreiter et al., 1998; Schrader et al., 1998; Li and Gould, 2002). The recently reported *PEX25* gene has also been implicated in the regulation of peroxisome size and number in *S. cerevisiae* (Smith et al., 2002), as has the dynamin-like protein Vps1p (Hoepfner et al., 2001). Like other dynamin-related proteins, Vps1p was proposed to be involved in a membrane fission event required for the regulation of peroxisome size and abundance. The thickened membranes between some peroxisomes of a peroxisome cluster seen in cells deleted for the *YHR150w* and/or *YDR479c* genes are also suggestive of a role for Yhr150p and Ydr479p in controlling fission of the peroxisomal membrane.

How might Yhr150p, Ydr479p, Pex11p, Pex25p, and Vps1p act and interact to control the abundance, size, and distribution of peroxisomes in the *S. cerevisiae* cell? We sought to get some insight into this question by determining the effects on peroxisome morphology of overexpressing the genes for these proteins in wild-type cells and cells deleted for the different genes.

Overexpression of the *PEX11* gene in the *pex11Δ* genetic background has been reported to result in large numbers of

The Journal of Cell Biology

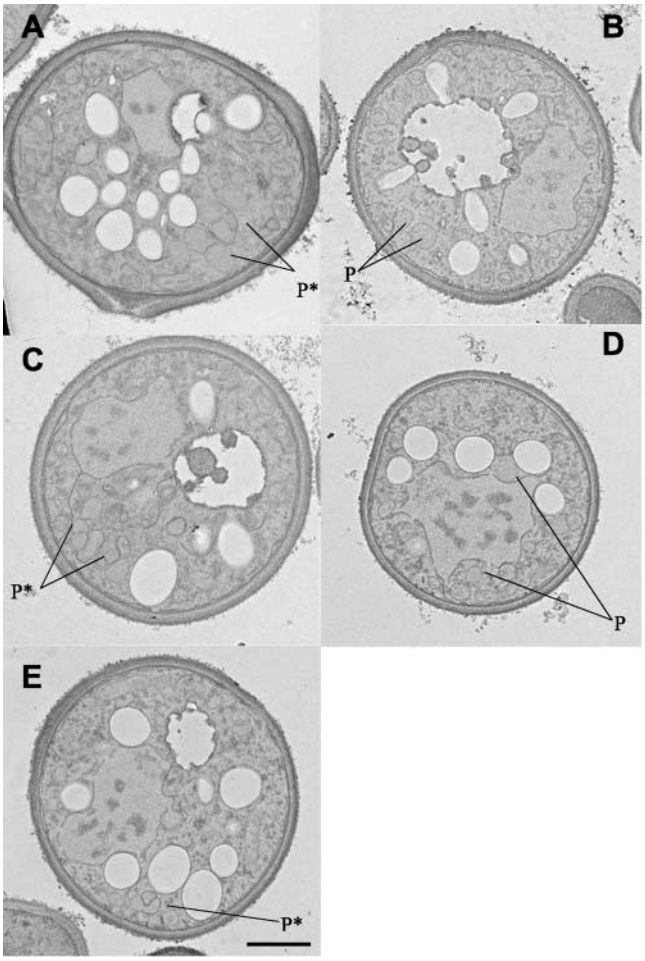

Figure 8. **Ultrastructure of *yhr150Δ/ydr479Δ* cells overexpressing *YHR150w, YDR479c, PEX11, PEX25,* or *VPS1*.** Cells of the *yhr150Δ/ydr479Δ* strain overexpressing *YHR150w* (A), *YDR479c* (B), *PEX11* (C), *PEX25* (D), or *VPS1* (E) were grown in SM medium overnight, transferred to YPBO medium, and incubated in YPBO medium for 8 h. P, peroxisome; P*, peroxisome cluster. Bar, 0.5 μm.

small peroxisomes (Marshall et al., 1995). In contrast, overexpression of *PEX25*, *VPS1*, *YHR150w*, and *YDR479c* in their respective gene deletion backgrounds does not result in the production of large numbers of small peroxisomes but instead restores the wild-type peroxisomal phenotype. Considering the proliferation of peroxisomes as a two-step pathway, namely division of peroxisomes and separation of peroxisomes, overexpression of the *PEX11* gene either in wild-type cells or in cells of the various deletion strains leads to a significant proliferation of peroxisomes, which remain, for the most part, adherent to one another. Thus, Pex11p plays a central and positive regulatory role in the division step of peroxisome proliferation but has little, or no readily apparent, role in the separation step of the process. The presence of reduced numbers of enlarged peroxisomes in *pex25Δ* (Smith et al., 2002; Fig. S1) and *vps1Δ* cells (Hoepfner et al., 2001; Fig. S1) suggests that Pex25p and Vps1p function, in addition to Pex11p, in the divisional step of peroxisome proliferation.

Upon completion of peroxisome division, peroxisomes must be separated from one another. Yhr150p and Ydr479p are two proteins required for this process, as their absence leads to an arrest or retardation of the peroxisome proliferation pathway, leading to the presence of clusters of peroxisomes with evidence of thickened membranes sometimes occurring between adjacent peroxisomes. Significant recovery of the wild-type peroxisomal phenotype by overexpression of *PEX25* or *VPS1* in cells deleted for one or both of the *YHR150w* or *YDR479c* genes implies that Pex25p and Vps1p have roles in the separation of peroxisomes in addition to their roles in peroxisome division discussed above. In contrast, overexpression of *PEX11* in cells deleted for one or both of the *YHR150w* or *YDR479c* genes did not result in the reappearance of wild-type peroxisomes, and peroxisomes remained clustered and sometimes exhibited membrane thickening between adjacent peroxisomes, as in the original strains deleted for *YHR150w* and/or *YDR479c*. Therefore, Pex11p appears to function primarily or only at the divisional step of peroxisome proliferation but not at the separation step.

Organelles are highly dynamic structures that undergo fission and fusion processes to allow cells to respond to intracellular and extracellular cues and to allow for their correct segregation at cell division. The maintenance of compartmental integrity in the eukaryotic cell, therefore, requires tight control mechanisms for these events. In the control of peroxisome number, size, and distribution, our data suggest that Pex11p plays a preeminent role in controlling peroxisome division, whereas Pex25p, Vps1p, and the newly identified peroxisomal proteins Yhr150p and Ydr479p all play a prominent role in controlling the separation of peroxisomes from one another. Because of their role in peroxisome dynamics, we suggest that *YHR150w* and *YDR479c* be designated as *PEX28* and *PEX29*, respectively, and their encoded peroxins as Pex28p and Pex29p. The challenge for the future lies in understanding further the interplay amongst these proteins and the signaling events they respond to and initiate in order to control peroxisomal dynamics in the cell.

Materials and methods

Strains and culture conditions

The yeast strains used in this study are listed in Table III. All strains were cultured at 30°C. Media components were as follows: YPD, 1% yeast extract, 2% peptone, 2% glucose; YPBO, 0.3% yeast extract, 0.5% peptone, 0.5% K_2HPO_4, 0.5% KH_2PO_4, 1% Brij 35, 1% (vol/vol) oleic acid; synthetic minimal (SM) medium, 0.67% yeast nitrogen base without amino acids, 2% glucose, 1× Complete Supplement Mixture (Bio 101) without histidine and/or leucine; sporulation medium, 1% potassium acetate, 0.1% yeast extract, 0.05% glucose, 2% agar; and YNBD, 0.67% yeast nitrogen base without amino acids, 2% glucose, containing histidine, leucine, and uracil, each at 30 μg/ml.

Plasmids

The plasmids pDsRed–PTS1 (Smith et al., 2002) and pProtA/HIS5 (Rout et al., 2000) have been previously described. Genes to be overexpressed were amplified by PCR and cloned into the plasmid YEp13 (Broach et al., 1979). For overexpression, the *YHR150w* gene included 492 bp of upstream and 398 bp of downstream sequence, the *YDR479c* gene included 642 bp of upstream and 335 bp of downstream sequence, the *PEX11* gene included 599 bp of upstream and 329 bp of downstream sequence, the *PEX25* gene included 753 bp of upstream and 319 bp of downstream sequence, and the *VPS1* gene included 555 bp of upstream and 324 bp of downstream sequence.

Protein A tagging of candidate proteins

Genes were genomically tagged with the sequence encoding *Staphylococcus aureus* protein A by homologous recombination using PCR-based inte-

The Journal of Cell Biology

Table III. **Yeast strains used in this study**

Organism	Strain	Genotype	Derivation
S. cerevisiae	*BY4741*	*MATa, his3Δ1, leu2Δ0, met15Δ0, ura3Δ0*	Giaever et al., 2002
	BY4742	*MATα, his3Δ1, leu2Δ0, lys2Δ0, ura3Δ0*	Giaever et al., 2002
	BY4743	*MATa/MATα, his3Δ1/his3Δ1, leu2Δ0/leu2Δ0, met15Δ0/+, +/lys2Δ0, ura3Δ0/ura3Δ0*	Giaever et al., 2002
	DF5α	*MATα, ura3-52, his3-200, trp1-1, leu2-3,112, lys2-801*	Finley et al., 1987
	DF5a	*MATa, ura3-52, his3-200, trp1-1, leu2-3,112, lys2-801*	Finley et al., 1987
	YDR479c-prA	*MATα, his3Δ1, leu2Δ0, lys2Δ0, ura3Δ0, ydr479c::YDR479c-protA (HIS5)*	This study
	YHR150w-prA	*MATα, his3Δ1, leu2Δ0, lys2Δ0, ura3Δ0, yhr150w::YHR150w-protA (HIS5)*	This study
	PEX3-prA	*MATα, his3Δ1, leu2Δ0, lys2Δ0, ura3Δ0, pex3::PEX3-protA (HIS5)*	This study
	PEX17-prA	*MATα, his3Δ1, leu2Δ0, lys2Δ0, ura3Δ0, pex17::PEX17-protA (HIS5)*	This study
	POT1-prA	*MATα, his3Δ1, leu2Δ0, lys2Δ0, ura3Δ0, pot1::POT1-protA (HIS5)*	This study
	TOM20-prA	*MATα, his3Δ1, leu2Δ0, lys2Δ0, ura3Δ0, tom20::TOM20-protA*	This study
	pex15Δ	*MATα, his3Δ1, leu2Δ0, lys2Δ0, ura3Δ0, pex15::KanMX4*	Giaever et al., 2002
	ydr479Δ	*MATα, his3Δ1, leu2Δ0, lys2Δ0, ura3Δ0, ydr479c::KanMX4*	Giaever et al., 2002
	yhr150Δ	*MATα, his3Δ1, leu2Δ0, lys2Δ0, ura3Δ0, yhr150w::KanMX4*	Giaever et al., 2002
	yhr150wΔ-A	*MATa, his3Δ1, leu2Δ1, met15Δ0, ura3Δ0, yhr150w::KanMX4*	This study
	yhr150wΔ-HD	*MATa/MATα, his3Δ1/his3Δ1, leu2Δ0/leu2Δ0, met15Δ0/+, +/lys2Δ0, ura3Δ0/ura3Δ0, yhr150w::KanMX4/+*	Giaever et al., 2002
	yhr150Δ/ydr479Δ	*MATa, his3Δ1, leu2Δ0, ura3Δ0, yhr150w::KanMX4, ydr479c::KanMX4*	This study
Y. lipolytica	*E122*	*MATA, ura3-302, leu2-270, lys8-11*	Tam and Rachubinski, 2002
	pex24KOA	*MATA, ura3-302, leu2-270, lys8-11, pex24::URA3*	Tam and Rachubinski, 2002

grative transformation into parental *BY4742* haploid cells (Aitchison et al., 1995; Dilworth et al., 2001).

Microscopy

Strains encoding protein A chimeras and transformed with the plasmid pDs-Red–PTS1 were grown in SM medium for 12 h and then incubated in YPBO medium for 8 h. Cells were processed for immunofluorescence microscopy as previously described (Pringle et al., 1991; Tam and Rachubinski, 2002). Protein A chimeras were detected with rabbit antiserum to mouse IgG (ICN Biomedicals) and FITC-conjugated goat anti–rabbit IgG. Images were captured on an LSM510 META (Carl Zeiss MicroImaging, Inc.) laser scanning microscope or with a digital fluorescence camera (Spot Diagnostic Instruments). Whole cells and subcellular fractions were processed for EM as previously described (Eitzen et al., 1997).

Morphometric analysis of peroxisomes

For each strain analyzed, electron micrographs of 50 randomly selected cells at a magnification of 17, 000 were scanned, and the areas of individual cells and of individual peroxisomes were determined by counting the number of individual pixels in a particular cell or peroxisome with Image Tool for Windows, Version 2.00 (University of Texas Health Science Center). To determine the average area of a peroxisome, the total peroxisome area was calculated and divided by the total number of peroxisomes counted. To quantify peroxisome number, the numerical density of peroxisomes (number of peroxisomes per μm^3 of cell volume) was calculated by the method of Weibel and Bolender (1973) for spherical organelles as follows. First, the total number of peroxisome profiles was counted and reported as the number of peroxisomes per cell area assayed (N_A). Next, the peroxisome volume density (V_V) was calculated for each strain (total peroxisome area/total cell area assayed). Using the values V_V and N_A, the numerical density of peroxisomes was determined (Weibel and Bolender, 1973).

Subcellular fractionation and isolation of peroxisomes

Subcellular fractionation and peroxisome isolation were done essentially as previously described (Bonifacino et al., 2000; Smith et al., 2002). In brief, cells grown overnight in YPD medium were transferred to YPBO medium and incubated for 8 h. Cells were harvested, washed, and converted to spheroplasts by digestion with Zymolyase 100T (1 mg/g of cells) in 50 mM potassium phosphate, pH 7.5, 1.2 M sorbitol, 1 mM EDTA for 1 h at 30°C. Spheroplasts were lysed by homogenization in buffer H (0.6 M sorbitol, 2.5 mM MES, pH 5.5, 1 mM KCl) containing 1 mM EDTA and PINS (0.5 mM benzamidine, 2 μg leupeptin/ml, 2 μg aprotinin/ml, 1 μg pepstatin A/ml, 3 μg antipain/ml, 0.5 mg Pefabloc/ml). The homogenate was subjected to centrifugation for 10 min at 2,000 *g* to yield a PNS fraction. The PNS fraction was subjected to further differential centrifugation at 20,000 *g* for 30 min to yield supernatant (20KgS) and pellet (20KgP) fractions. The 20KgP fraction was resuspended in buffer H containing 11% Nycodenz and PINS, and a volume containing 5 mg of protein was overlaid onto either a 30-ml discontinuous gradient consisting of 17, 25, 35, and 50% (wt/vol) Nycodenz or a 30-ml continuous gradient of 30–45% (wt/vol) Nycodenz, both in buffer H containing PINS. Organelles were separated by centrifugation at 100,000 *g* for 90 min in a VTi50 rotor (Beckman Coulter). Fractions of 2 ml were collected from the bottom of the gradient.

Extraction of peroxisomes

Peroxisomes were extracted as previously described (Fujiki et al., 1982; Nuttley et al., 1990). Essentially, organelles in the 20KgP fraction (50 μg of protein) were lysed by incubation in 10 volumes of Ti8 buffer (10 mM Tris-HCl, pH 8.0) containing 3× PINS on ice for 1 h and separated into pellet (Ti8P) and supernatant (Ti8S) fractions by centrifugation at 245,000 *g* for 1 h at 4°C in a TLA120.2 rotor (Beckman Coulter). The Ti8P fraction was resuspended in Ti8 buffer to a final protein concentration of 0.5 mg/ml, and a portion of the resuspended fraction was extracted with 0.1 M Na_2CO_3, pH 11.3, for 1 h on ice and then separated into supernatant (CO_3S) and pellet (CO_3P) fractions by centrifugation at 245,000 *g* in a TLA120.2 rotor at 4°C for 1 h. Proteins in the Ti8S, Ti8P, CO_3S, and CO_3P fractions were precipitated by addition of TCA, and the precipitates were washed with acetone. Proteins in equal portions of each fraction were separated by SDS-PAGE and analyzed by immunoblotting.

Construction of a haploid strain deleted for both the *YDR479c* and *YHR150w* genes

The homozygous deletion diploid strain *yhr150wΔ-HD* (Giaever et al., 2002) was sporulated, and the tetrads were dissected to select for the haploid *MATa* strain. This strain was mated to the haploid *MATα* deletion strain *ydr479cΔ* by replica plating to obtain a heterozygous diploid strain harboring deletions for both *YHR150w* and *YDR479c*. The diploid strain was sporulated, and tetrads from 10 heterozygous diploids were dissected by micromanipulation. All spores were grown in YPD medium, and DNA was extracted. Haploid strains carrying deletions in both the *YDR479c* and *YHR150w* genes were selected by PCR analysis.

Antibodies

Antibodies to the carboxy-terminal SKL tripeptide (Aitchison et al., 1992), thiolase (Eitzen et al., 1996), and Sdh2p (Dibrov et al., 1998) have been previously described. FITC-conjugated anti–rabbit IgG and rhodamine-conjugated anti–guinea pig IgG (Jackson ImmunoResearch Laboratories) were used to detect primary antibodies in immunofluorescence microscopy. Rabbit antibodies to glucose-6-phosphate dehydrogenase (G6PDH) of *S. cerevisiae* were obtained from Sigma-Aldrich.

The Journal of Cell Biology

The Journal of Cell Biology

Analytical procedures

Extraction of nucleic acid from yeast lysates and manipulation of DNA were performed as previously described (Ausubel et al., 1994). Immunoblotting was performed using a wet transfer system (Ausubel et al., 1994), and antigen–antibody complexes in immunoblots were detected by ECL (Amersham Biosciences). Protein concentration was determined using a commercially available kit (Bio-Rad Laboratories) and bovine serum albumin as a standard.

Online supplemental material

The online version of this manuscript (http://www.jcb.org/cgi/content/full/jcb.200210130/DC1) contains additional figures (Figs. S1–S6) showing the ultrastructure of cells of the gene deletion strains *pex11Δ*, *pex15Δ*, *pex25Δ*, and *vps1Δ* and of various strains overexpressing the *YHR150w*, *YDR479c*, *PEX11*, *PEX25*, and *VPS1* genes. Cells were grown overnight in glucose-containing medium, transferred to oleic acid–containing medium, and incubated in oleic acid–containing medium for 8 h. Cells were then fixed and processed for EM.

We thank Honey Chan for her expert assistance with EM and Richard Poirier for help with confocal microscopy.

This work was supported by operating grant 39322 from the Canadian Institutes of Health Research to R.A. Rachubinski and J.D. Aitchison. R.A. Rachubinski holds the Canada Research Chair in Cell Biology and is an International Research Scholar of the Howard Hughes Medical Institute. Y.Y.C. Tam is the recipient of a studentship from the Alberta Heritage Foundation for Medical Research.

Submitted: 23 October 2002
Revised: 4 March 2003
Accepted: 10 March 2003

References

Abe, I., and Y. Fujiki. 1998. cDNA cloning and characterization of a constitutively expressed isoform of the human peroxin Pex11p. *Biochem. Biophys. Res. Commun.* 252:529–533.

Aitchison, J.D., W.W. Murray, and R.A. Rachubinski. 1991. The carboxyl-terminal tripeptide Ala-Lys-Ile is essential for targeting *Candida tropicalis* trifunctional enzyme to yeast peroxisomes. *J. Biol. Chem.* 266:23197–23203.

Aitchison, J.D., R.K. Szilard, W.M. Nuttley, and R.A. Rachubinski. 1992. Antibodies directed against a yeast carboxyl-terminal peroxisomal targeting signal specifically recognize peroxisomal proteins from various yeasts. *Yeast.* 8:721–734.

Aitchison, J.D., M.P. Rout, M. Marelli, G. Blobel, and R.W. Wozniak. 1995. Two novel related yeast nucleoporins Nup170p and Nup157p: complementation with the vertebrate homologue Nup155p and functional interactions with the yeast nuclear pore-membrane protein Pom152p. *J. Cell Biol.* 131:1133–1148.

Ausubel, F.M., R. Brent, R.E. Kingston, D.D. Moore, J.G. Seidman, J.A. Smith, and K. Struhl. 1994. Current Protocols in Molecular Biology. John Wiley & Sons, New York.

Bonifacino, J.S., M. Dasso, J. Lippincott-Schwartz, J.B. Harford, and K.M. Yamada. 2000. Isolation of oleate-induced peroxisomes using sucrose gradient step gradients. *In* Current Protocols in Cell Biology. John Wiley & Sons, New York. 3.8.32–3.8.36.

Broach, J.R., J.N. Strathern, and J.B. Hicks. 1979. Transformation in yeast: development of a hybrid cloning vector and isolation of the *CAN1* gene. *Gene.* 8:121–133.

Brosius, U., and J. Gärtner. 2002. Cellular and molecular aspects of Zellweger syndrome and other peroxisome biogenesis disorders. *Cell. Mol. Life Sci.* 59: 1058–1069.

Chang, C.C., S. South, D. Warren, J. Jones, A.B. Moser, H.W. Moser, and S.J. Gould. 1999. Metabolic control of peroxisome abundance. *J. Cell Sci.* 112: 1579–1590.

Dammai, V., and S. Subramani. 2001. The human peroxisomal targeting signal receptor, Pex5p, is translocated into the peroxisomal matrix and recycled to the cytosol. *Cell.* 105:187–196.

Dibrov, E., S. Fu, and B.D. Lemire. 1998. The *Saccharomyces cerevisiae TCM62* gene encodes a chaperone necessary for the assembly of the mitochondrial succinate dehydrogenase (complex II). *J. Biol. Chem.* 273:32042–32048.

Dilworth, D.J., A. Suprapto, J.C. Padovan, B.T. Chait, R.W. Wozniak, M.P. Rout, and J.D. Aitchison. 2001. Nup2p dynamically associates with the distal regions of the yeast nuclear pore complex. *J. Cell Biol.* 153:1465–1478.

Dyer, J.M., J.A. McNew, and J.M. Goodman. 1996. The sorting sequence of the peroxisomal integral membrane protein PMP47 is contained within a short hydrophilic loop. *J. Cell Biol.* 133:269–280.

Eitzen, G.A., V.I. Titorenko, J.J. Smith, M. Veenhuis, R.K. Szilard, and R.A. Rachubinski. 1996. The *Yarrowia lipolytica* gene *PAY5* encodes a peroxisomal integral membrane protein homologous to the mammalian peroxisome assembly factor PAF-1. *J. Biol. Chem.* 271:20300–20306.

Eitzen, G.A., R.K. Szilard, and R.A. Rachubinski. 1997. Enlarged peroxisomes are present in oleic acid–grown *Yarrowia lipolytica* overexpressing the *PEX16* gene encoding an intraperoxisomal peripheral membrane peroxin. *J. Cell Biol.* 137:1265–1278.

Elgersma, Y., C.W. van Roermund, R.J. Wanders, and H.F. Tabak. 1995. Peroxisomal and mitochondrial carnitine acetyltransferases of *Saccharomyces cerevisiae* are encoded by a single gene. *EMBO J.* 14:3472–3479.

Elgersma, Y., L. Kwast, M. van den Berg, W.B. Snyder, B. Distel, S. Subramani, and H.F. Tabak. 1997. Overexpression of Pex15p, a phosphorylated peroxisomal integral membrane protein required for peroxisome assembly in *S. cerevisiae*, causes proliferation of the endoplasmic reticulum membrane. *EMBO J.* 16:7326–7341.

Erdmann, R., and G. Blobel. 1995. Giant peroxisomes in oleic acid–induced *Saccharomyces cerevisiae* lacking the peroxisomal membrane protein Pmp27p. *J. Cell Biol.* 128:509–523.

Fan, C.-Y., J. Pan, N. Usuda, A.V. Yeldandi, M.S. Rao, and J.K. Reddy. 1998. Steatohepatitis, spontaneous peroxisome proliferation and liver tumors in mice lacking peroxisomal fatty acyl-CoA oxidase. Implications for peroxisome proliferator-activated receptor α natural ligand metabolism. *J. Biol. Chem.* 273:15639–15645.

Finley, D., E. Ozkaynak, and A. Varshavsky. 1987. The yeast polyubiquitin gene is essential for resistance to high temperatures, starvation, and other stresses. *Cell.* 48:1035–1046.

Fujiki, Y. 2000. Peroxisome biogenesis and peroxisome biogenesis disorders. *FEBS Lett.* 476:42–46.

Fujiki, Y., A.L. Hubbard, S. Fowler, and P.B. Lazarow. 1982. Isolation of intracellular membranes by means of sodium carbonate treatment: application to endoplasmic reticulum. *J. Cell Biol.* 93:97–102.

Giaever, G., A.M. Chu, L. Ni, C. Connelly, L. Riles, S. Véronneau, S. Dow, A. Lucau-Danila, K. Anderson, B. André, et al. 2002. Functional profiling of the *Saccharomyces cerevisiae* genome. *Nature.* 418:387–391.

Glover, J.R., D.W. Andrews, and R.A. Rachubinski. 1994a. *Saccharomyces cerevisiae* peroxisomal thiolase is imported as a dimer. *Proc. Natl. Acad. Sci. USA.* 91:10541–10545.

Glover, J.R., D.W. Andrews, S. Subramani, and R.A. Rachubinski. 1994b. Mutagenesis of the amino targeting signal of *Saccharomyces cerevisiae* 3-ketoacyl-CoA thiolase reveals conserved amino acids required for import into peroxisomes in vivo. *J. Biol. Chem.* 269:7558–7563.

Gould, S.J., and D. Valle. 2000. Peroxisome biogenesis disorders: genetics and cell biology. *Trends Genet.* 16:340–345.

Gould, S.J., G.-A. Keller, and S. Subramani. 1987. Identification of a peroxisomal targeting signal at the carboxy terminus of firefly luciferase. *J. Cell Biol.* 105: 2923–2931.

Gould, S.J., G.-A. Keller, N. Hosken, J. Wilkinson, and S. Subramani. 1989. A conserved tripeptide sorts proteins to peroxisomes. *J. Cell Biol.* 108:1657–1664.

Gould, S.J., S. Krisans, G.-A. Keller, and S. Subramani. 1990. Antibodies directed against the peroxisomal targeting signal of firefly luciferase recognize multiple mammalian peroxisomal proteins. *J. Cell Biol.* 110:27–34.

Hettema, E.H., B. Distel, and H.F. Tabak. 1999. Import of proteins into peroxisomes. *Biochim. Biophys. Acta.* 1451:17–34.

Hoepfner, D., M. van den Berg, P. Philippsen, H.F. Tabak, and E.H. Hettema. 2001. A role for Vps1p, actin, and the Myo2p motor in peroxisome abundance and inheritance in *Saccharomyces cerevisiae. J. Cell Biol.* 155:979–990.

Höhfeld, J., M. Veenhuis, and W.-H. Kunau. 1991. PAS3, a *Saccharomyces cerevisiae* gene encoding a peroxisomal integral membrane protein essential for peroxisome biogenesis. *J. Cell Biol.* 114:1167–1178.

Huhse, B., P. Rehling, M. Albertini, L. Blank, K. Meller, and W.-H. Kunau. 1998. Pex17p of *Saccharomyces cerevisiae* is a novel peroxin and component of the peroxisomal protein translocation machinery. *J. Cell Biol.* 140:49–60.

Kragler, F., A. Langeder, J. Raupachova, M. Binder, and A. Hartig. 1993. Two independent peroxisomal targeting signals in catalase A of *Saccharomyces cerevisiae. J. Cell Biol.* 120:665–673.

Krogh, A., B. Larsson, G. von Heijne, and E.L.L. Sonnhammer. 2001. Predicting transmembrane protein topology with a hidden Markov model: application to complete genomes. *J. Mol. Biol.* 305:567–580.

Lazarow, P.B., and Y. Fujiki. 1985. Biogenesis of peroxisomes. *Annu. Rev. Cell*

Biol. 1:489–530.

Lazarow, P.B., and H.W. Moser. 1994. Disorders of peroxisome biogenesis. *In* The Metabolic Basis of Inherited Disease. A.L. Beaudet, W.S. Sly, and A.D. Valle, editors. McGraw-Hill Inc., New York. 2287–2324.

Li, X., and S.J. Gould. 2002. PEX11 promotes peroxisome division independently of peroxisome metabolism. *J. Cell Biol.* 156:643–651.

Lithgow, T., T. Junne, C. Wachter, and G. Schatz. 1994. Yeast mitochondria lacking the two import receptors Mas20p and Mas70p can efficiently and specifically import precursor proteins. *J. Biol. Chem.* 269:15325–15330.

Lorenz, P., A.G. Maier, E. Baumgart, R. Erdmann, and C. Clayton. 1998. Elongation and clustering of glycosomes in *Trypanosoma brucei* overexpressing the glycosomal Pex11p. *EMBO J.* 17:3542–3555.

Marshall, P.A., Y.I. Krimkevich, R.H. Lark, J.M. Dyer, M. Veenhuis, and J.M. Goodman. 1995. Pmp27 promotes peroxisomal proliferation. *J. Cell Biol.* 129:345–355.

Marshall, P.A., J.M. Dyer, M.E. Quick, and J.M. Goodman. 1996. Redox-sensitive homodimerization of Pex11p: a proposed mechanism to regulate peroxisomal division. *J. Cell Biol.* 135:123–137.

McCammon, M.T., J.A. McNew, P.J. Willy, and J.M. Goodman. 1994. An internal region of the peroxisomal membrane protein PMP47 is essential for sorting to peroxisomes. *J. Cell Biol.* 124:915–925.

McNew, J.A., and J.M. Goodman. 1994. An oligomeric protein is imported into peroxisomes in vivo. *J. Cell Biol.* 127:1245–1257.

Nuttley, W.M., A.G. Bodnar, D. Mangroo, and R.A. Rachubinski. 1990. Isolation and characterization of membranes from oleic acid-induced peroxisomes of *Candida tropicalis. J. Cell Sci.* 95:463–470.

Osumi, T., T. Tsukamoto, S. Hata, S. Yokota, S. Miura, Y. Fujiki, M. Hijikata, S. Miyazawa, and T. Hashimoto. 1991. Amino-terminal presequence of the precursor of peroxisomal 3-ketoacyl-CoA thiolase is a cleavable signal peptide for peroxisomal targeting. *Biochem. Biophys. Res. Commun.* 181:947–954.

Passreiter, M., M. Anton, D. Lay, R. Frank, C. Harter, F.T. Wieland, K. Gorgas, and W.W. Just. 1998. Peroxisome biogenesis: involvement of ARF and coatomer. *J. Cell Biol.* 141:373–383.

Pause, B., R. Saffrich, A. Hunziker, W. Ansorge, and W.W. Just. 2000. Targeting of the 22 kDa integral peroxisomal membrane protein. *FEBS Lett.* 471:23–28.

Pringle, J.R., A.E.M. Adams, D.G. Drubin, and B.K. Haarer. 1991. Immunofluorescence methods for yeasts. *Methods Enzymol.* 194:565–602.

Purdue, P.E., and P.B. Lazarow. 2001. Peroxisome biogenesis. *Annu. Rev. Cell Dev. Biol.* 17:701–752.

Purdue, P.E., Y. Takada, and C.J. Danpure. 1990. Identification of mutations associated with peroxisome-to-mitochondrion mistargeting of alanine/glyoxylate aminotransferase in primary hyperoxaluria type 1. *J. Cell Biol.* 111: 2341–2351.

Rout, M.P., J.D. Aitchison, A. Suprapto, K. Hjertaas, Y. Zhao, and B.T. Chait. 2000. The yeast nuclear pore complex: composition, architecture, and transport mechanism. *J. Cell Biol.* 148:635–651.

Sakai, Y., P.A. Marshall, A. Saiganji, K. Takabe, H. Saiki, N. Kato, and J.M. Goodman. 1995. The *Candida boidinii* peroxisomal membrane protein Pmp30 has a role in peroxisomal proliferation and is functionally homologous to Pmp27 from *Saccharomyces cerevisiae. J. Bacteriol.* 177:6773–6781.

Schrader, M., B.E. Reuber, J.C. Morrell, G. Jimenez-Sanchez, C. Obie, T.A. Stroh, D. Valle, T.A. Schroer, and S.J. Gould. 1998. Expression of Pex11β mediates peroxisome proliferation in the absence of extracellular stimuli. *J. Biol. Chem.* 273:29607–29614.

Small, G.M., L.J. Szabo, and P.B. Lazarow. 1988. Acyl-CoA oxidase contains two targeting sequences each of which can mediate protein import into peroxisomes. *EMBO J.* 7:1167–1173.

Smith, J.J., T.W. Brown, G.A. Eitzen, and R.A. Rachubinski. 2000. Regulation of peroxisome size and number by fatty acid β-oxidation in the yeast *Yarrowia lipolytica. J. Biol. Chem.* 275:20168–20178.

Smith, J.J., M. Marelli, R.H. Christmas, F.J. Vizeacoumar, D.J. Dilworth, T. Ideker, T. Galitski, K. Dimitrov, R.A. Rachubinski, and J.D. Aitchison. 2002. Transcriptome profiling to identify genes involved in peroxisome assembly and function. *J. Cell Biol.* 158:259–271.

Subramani, S. 1993. Protein import into peroxisomes and biogenesis of the organelle. *Annu. Rev. Cell Biol.* 9:445–478.

Subramani, S. 1998. Components involved in peroxisome import, biogenesis, proliferation, turnover, and movement. *Physiol. Rev.* 78:171–188.

Subramani, S., A. Koller, and W.B. Snyder. 2000. Import of peroxisomal matrix and membrane proteins. *Annu. Rev. Biochem.* 69:399–418.

Swinkels, B.W., S.J. Gould, A.G. Bodnar, R.A. Rachubinski, and S. Subramani. 1991. A novel, cleavable peroxisomal targeting signal at the amino-terminus of the rat 3-ketoacyl-CoA thiolase. *EMBO J.* 10:3255–3262.

Swinkels, B.W., S.J. Gould, and S. Subramani. 1992. Targeting efficiencies of various permutations of the consensus C-terminal tripeptide peroxisomal targeting signal. *FEBS Lett.* 305:133–136.

Tam, Y.Y.C., and R.A. Rachubinski. 2002. *Yarrowia lipolytica* cells mutant for the *PEX24* gene encoding a peroxisomal membrane peroxin mislocalize peroxisomal proteins and accumulate membrane structures containing both peroxisomal matrix and membrane proteins. *Mol. Biol. Cell.* 13:2681–2691.

Terlecky, S.R., and M. Fransen. 2000. How peroxisomes arise. *Traffic.* 1:465–473.

Titorenko, V.I., J.-M. Nicaud, H. Wang, H. Chan, and R.A. Rachubinski. 2002. Acyl-CoA oxidase is imported as a heteropentameric, cofactor-containing complex into peroxisomes of *Yarrowia lipolytica. J. Cell Biol.* 156:481–494.

Titorenko, V.I., and R.A. Rachubinski. 2001. The life cycle of the peroxisome. *Nat. Rev. Mol. Cell Biol.* 2:357–368.

Titorenko, V.I., J.J. Smith, R.K. Szilard, and R.A. Rachubinski. 1998. Pex20p of the yeast *Yarrowia lipolytica* is required for the oligomerization of thiolase in the cytosol and for its targeting to the peroxisome. *J. Cell Biol.* 142:403–420.

van den Bosch, H., R.B.H. Schutgens, R.J.A. Wanders, and J.M. Tager. 1992. Biochemistry of peroxisomes. *Annu. Rev. Biochem.* 61:157–197.

van Roermund, C.W.T., H.F. Tabak, M. van den Berg, R.J.A. Wanders, and E.H. Hettema. 2000. Pex11p plays a primary role in medium-chain fatty acid oxidation, a process that affects peroxisome number and size in *Saccharomyces cerevisiae. J. Cell Biol.* 150:489–497.

Walton, P.A., S.J. Gould, J.R. Feramisco, and S. Subramani. 1992. Transport of microinjected proteins into peroxisomes of mammalian cells: inability of Zellweger cell lines to import proteins with the SKL tripeptide peroxisomal targeting signal. *Mol. Cell. Biol.* 12:531–541.

Walton, P.A., P.E. Hill, and S. Subramani. 1995. Import of stably folded proteins into peroxisomes. *Mol. Biol. Cell.* 6:675–683.

Waterham, H.R., V.I. Titorenko, P. Haima, J.M. Cregg, W. Harder, and M. Veenhuis. 1994. The *Hansenula polymorpha PER1* gene is essential for peroxisome biogenesis and encodes a peroxisomal matrix protein with both carboxy- and amino-terminal targeting signals. *J. Cell Biol.* 127:737–749.

Weibel, E.R., and P. Bolender. 1973. Stereological techniques for electron microscopic morphometry. *In* Principles and Techniques of Electron Microscopy. Vol. 3. M.A. Hayat, editor. Van Nostrand Reinhold, New York. 237–296.

The Journal of Cell Biology